NeuroImage: Clinical 4 (2014) 201–208

Contents lists available at ScienceDirect

NeuroImage: Clinical

journal homepage: www.elsevier.com/locate/ynicl

Motor recovery and microstructural change in rubro-spinal tract in subcortical stroke ☆

Yohei Takenobu [a,b], Takuya Hayashi [b,c,*], Hiroshi Moriwaki [a,d], Kazuyuki Nagatsuka [a], Hiroaki Naritomi [a,1], Hidenao Fukuyama [b]

[a] Division of Neurology, Department of Stroke and Cerebrovascular Diseases, National Cerebral and Cardiovascular Center, Osaka, Japan
[b] Human Brain Research Center, Kyoto University Graduate School of Medicine, Kyoto, Japan
[c] Functional Architecture Imaging Unit, RIKEN Center for Life Science Technologies, Kobe, Japan
[d] Department of Neurology, Kansai Rosai Hospital, Hyogo, Japan

ARTICLE INFO

Article history:
Received 18 October 2013
Received in revised form 2 December 2013
Accepted 5 December 2013
Available online 13 December 2013

Keywords:
Motor recovery
Subcortical stroke
Reorganization
Diffusion tensor image
Tract-based spatial statistics

ABSTRACT

The mechanism of motor recovery after stroke may involve reorganization of the surviving networks. However, details of adaptive changes in structural connectivity are not well understood. Here, we show long-term changes in white matter microstructure that relate to motor recovery in stroke patients. We studied ten subcortical ischemic stroke patients who showed motor hemiparesis at the initial clinical examination and an infarcted lesion centered in the posterior limb of internal capsule of the unilateral hemisphere at the initial diffusion-weighted magnetic resonance imaging scan. The participants underwent serial diffusion tensor imaging and motor function assessments at three consecutive time points; within 2 weeks, and at 1 and 3 months after the onset. Fractional anisotropy (FA) was analyzed for regional differences between hemispheres and time points, as well as for correlation with motor recovery using a tract-based spatial statistics analysis. The results showed significantly increased FA in the red nucleus and dorsal pons in the ipsi-lesional side at 3 months, and significantly decreased FA in the ipsi-lesional internal capsule at all time points, and in the cerebral peduncle, corona radiata, and corpus callosum at 3 months. In the correlation analysis, FA values of clusters in the red nucleus, dorsal pons, midbody of corpus callosum, and cingulum were positively correlated with recovery of motor function. Our study suggests that changes in white matter microstructure in alternative descending motor tracts including the rubro-spinal pathway, and interhemispheric callosal connections may play a key role in compensating for motor impairment after subcortical stroke.

1. Introduction

Stroke is the leading cause of adult-onset disabilities, and hemiparesis is among the strongest predictors of later activity of daily life (Veerbeek et al., 2011). Accumulating evidence shows that patients can make a significant recovery from motor disabilities during the initial 3 months after the onset of stroke (Duncan et al., 1992; Kelly-Hayes et al., 1989). Neuroimaging studies have recently elucidated part of the mechanism that accounts for functional recovery after stroke (see Grefkes and Ward, in press); however, details of reorganization by the surviving network are not fully understood. In animal studies, the extrapyramidal descending tract (EPT) including rubro-spinal and reticulo-spinal pathways (Lemon, 2008), a phylogenetically old corticofugal system, plays a role in recovering motor function after pyramidal tract (PT) injury (Belhaj-Saïf and Cheney, 2000; Lawrence and Kuypers, 1968; Zaaimi et al., 2012). However, in humans, there is sparse evidence for anatomical and functional significance of the EPT system (Baker, 2011; Lemon, 2008), or for its role in motor recovery.

Diffusion tensor imaging (DTI) allows us to estimate micro-architectural changes of the white matter and neuronal fiber bundles (Basser et al., 1994). Obtained DTI measures are able to quantitatively detect experimental degeneration of white matter tracts (Hayashi et al., 2013) and are also associated with the degree of motor dysfunction in stroke (Lindenberg et al., 2010; Stinear et al., 2007). Recently, Lindenberg et al. (2010) suggested that the outcome of motor impairment in stroke can be better predicted by microstructural changes of the PT and EPT together than changes of the PT alone. Additionally, others reported increased fractional anisotropy in the rubro-spinal

Abbreviations: CC, Corpus callosum; CP, Cerebral peduncle; CR, Corona radiata; DTI, Diffusion tensor imaging; EPT, Extrapyramidal tract; FA, Fractional Anisotropy; FMMS, Fugl-Meyer Motor Scale; PLIC, Posterior limb of internal capsule; PT, Pyramidal tract; TBSS, Tract-based spatial statistics.

* Corresponding author at: Functional Architecture Imaging Unit, RIKEN Center for Life Science Technologies, 6-7-3 Minatojima-minamimachi, Chuo-ku, Kobe, Hyogo 650-0047, Japan. Tel.: +81 78 304 7140; fax: +81 78 304 7141.
E-mail address: takuya.hayashi@riken.jp (T. Hayashi).
[1] Present addresses: Department of Neurology, Senri Chuo Hospital, Osaka, Japan.

2213-1582/$ – see front matter © 2013 The Authors. Published by Elsevier Inc. All rights reserved.
http://dx.doi.org/10.1016/j.nicl.2013.12.003

pathway, part of the EPT system, in chronic stroke patients (Rüber et al., 2012; Yeo and Jang, 2010). However, these cross-sectional studies cannot evaluate longitudinal changes in the EPT system or motor function.

In the present study, we hypothesized that 1) microstructure of the regional white matter would change across time and hemispheres after stroke, and 2) if microstructural change was present, increase in fractional anisotropy would be associated with recovery of motor function. We show longitudinal changes of the white matter microstructure in subcortical stroke patients during a 3-month period, which are correlated with serially improved motor function.

2. Materials and methods

2.1. Patients

Ten patients with acute ischemic stroke, admitted to the Stroke Care Unit at the National Cerebral and Cardiovascular Research Center, were enrolled in this study. On admission the patients presented with minor to moderate impairment varying from 3 to 11 (median = 4.5) on the National Institute of Health Stroke Scale (NIHSS) and fulfilled the following inclusion criteria: (1) aged 20 years or more; (2) first-ever stroke of supratentorial pyramidal tract infarction; (3) presence of hemiparesis; and (4) clinically stable and first magnetic resonance imaging (MRI) scan acquired within 2 weeks of onset. Exclusion criteria were the presence of any cortical ischemic lesion and previous infarcted lesion involving pyramidal tracts in the initial MRI scan, disturbance of consciousness, neurological symptoms suggesting a cortical lesion (hemispatial agnosia or neglect, aphasia, apraxia), or the presence of other neurological and psychiatric disorders. We also assessed the initial T2-weighted MRI image for chronic white matter lesions using the Fazekas grade of periventricular and deep white matter hyperintensity (Fazekas et al., 1987). The study protocol was approved by the Institutional Review Board (M19-12), and was conducted in accordance with the Declaration of Helsinki and all patients gave written informed consent to participate in this study.

Each patient underwent serial examinations for neurological symptoms as well as for diffusion tensor MR imaging at 3 time points: within 2 weeks (Scan 1), at 1 month (Scan 2), and at 3 months (Scan 3) following stroke onset. Neurological motor symptoms were scored on the Fugl-Meyer Motor Scale (FMMS) (Gladstone et al., 2002), which has a range of 0 (complete hemiplegia) to 100 (normal performance) and consists of scores for upper extremities (= 66) and for lower extremities (= 34), during a comprehensive neurological examination by a board-certified neurologist (Y.T.). During the follow-up, all patients received standard medical treatment and rehabilitation, and no patient received thrombolysis, thrombectomy, or experimental treatment.

2.2. MR data acquisition

MR images were acquired with a 3 T whole-body MRI scanner (Signa3.0, GE Healthcare, Milwaukee, WI, USA) using a 16-channel phased-array head coil. Participants were placed on the scanner gantry in a head-first supine position with their ears plugged and heads secured by a plastic holder to minimize movements. The DTI data were obtained with a single-shot echo-planar imaging sequence [repetition time (TR)/echo time (TE) = 16,000/72.1 ms; flip angle = 90°; field of view (FOV) = 256 mm; matrix size = 128 × 128; slice thickness = 2 mm; 70 contiguous axial slices covering the entire brain], which consisted of 81 volumes with non-collinear diffusion gradient directions and a b-value of 1000 s/mm^2, and 9 volumes with a b-value of 0 s/mm^2. We also obtained T1- and T2-weighted MRI scans for structural information and lesion localization, as well as a gradient-echo type field map for correcting distortion in the DTI data. The entire scanning session took around 60 min and was tolerated by all subjects.

2.3. Data preprocessing

MRI data were analyzed using FMRIB Software Library (FSL) 4.1.8 (http://www.fmrib.ox.ac.uk/fsl) (Jenkinson et al., 2012), developed by the Centre for Functional Magnetic Resonance Imaging of the Brain, Oxford, UK. The DTI data were preprocessed for brain extraction, distortion corrected using the field map data, eddy-current distortion corrected with an affine transformation, and analyzed by fitting a diffusion tensor model (Basser et al., 1994) to generate a fractional anisotropy (FA) image. The FA images were fed into statistics across sessions and patients by a voxel-based spatial statistics method, as well as by a region-of-interest (ROI) method as described below.

2.4. Tract-based spatial statistics (TBSS)

Voxel-based statistical analysis of FA images was carried out using Tract-Based Spatial Statistics (TBSS), part of FSL (Smith et al., 2006). All subjects' FA maps were non-linearly warped to generate an averaged symmetric FA image in the Montreal Neurological Institute (MNI) space using a non-linear image registration tool (FMRIB's Non-linear Image Registration Tool, FNIRT). To avoid shrinkage of the lesion area during the warping process, we used an infarcted lesion area map (generated as described below) as a mask to exclude from warping. The values in the warped FA images were projected onto the FA skeleton, which represents the centers of fiber bundles (Smith et al., 2006). Before this projection, warped FA images for the patients who were affected in the right hemisphere (patients 3, 4, 7, and 8, see Table 1) were right-to-left flipped to align the lesion side to the contralateral to allow us to use voxel-based statistics across all the subjects. The resulting data in the FA skeleton of the MNI space were fed into voxel-wise statistics for cross-scan and cross-subject analyses. We performed three statistical analyses using FA data as a dependent variable for (1) within-subject interhemispheric difference using a paired *t*-test for each time point separately (Scans 1–3); (2) the effect of time by a paired *t*-test between a pair of three sessions; and (3) correlation with FMMS scores. For analyzing interhemispheric differences [analysis (1)], we performed a right–left flip for all the warped images and compared between non-flipped and flipped images. In the correlation analysis [analysis (3)], we used FA data from all sessions, and the FMMS score at the corresponding point, with scores demeaned within subjects. Statistics were performed with a nonparametric permutation test using 5000 Monte Carlo simulations. The statistical threshold was set at a family-wise error corrected $p < 0.05$, based on the threshold-free cluster enhancement (TFCE) method (Smith and Nichols, 2009). The anatomical locations of significant clusters were denominated based on the atlas of JHU ICBM-DTI-81 White Matter Labels, part of the FSL atlas tools (Mori and Crain, 2005), and on Witelson's callosal atlas (Witelson, 1989).

We also performed a ROI analysis for significant clusters found in the TBSS to look at the details of FA change. Our interest was in each of the clusters in the TBSS analysis and in its corresponding mirrored region, both in the standard space. We obtained FA values of ROIs from each subject's image in the native space, and tested for the effect of hemisphere and scan session using a repeated measure analysis of variance (ANOVA), as well as for the correlation with FMMS scores. ROIs in the standard space were warped to the subject's native space by inverting the nonlinear registration. For the cluster in the corona radiata (CR), ROIs in the native space obtained as above were overlapped with infarcted areas (see described below) in some subjects, thus we obtained FA values only from voxels that did not include the infarcted area.

Table 1
Patients' characteristics.

Patient no.	Age	Sex	Lesion location	Lesion volume (cm^3)	NIHSS score on admission	Fazekas grade		Post-onset days			FMMS score		
						PVH	DWMH	Scan 1	Scan 2	Scan 3	Scan 1	Scan 2	Scan 3
1	57	M	L PLIC	0.77	5	2	2	12	38	95	68	76	92
2	71	M	L CR/PLIC	8.8	11	2	2	4	46	95	9	9	22
3	73	M	R CR	2.4	6	1	1	10	45	101	56	63	79
4	77	M	R PLIC	0.27	3	1	0	5	28	92	82	88	93
5	76	M	L PLIC	0.62	4	2	2	7	26	82	72	88	92
6	70	M	L PLIC	0.41	3	3	3	12	40	96	79	88	92
7	81	M	R CR	1.1	7	3	3	7	34	95	49	65	73
8	76	M	R PLIC	0.73	4	2	2	9	36	99	76	85	91
9	74	F	L PLIC	0.58	3	1	1	14	41	91	79	89	93
10	72	M	L PLIC	0.83	5	1	1	12	41	100	62	76	82
Mean	72.7			1.7	4.5[a]	2[a]	2[a]	9.2	37.6	94.9	63.2	72.7	80.9
SD	6.4			2.6				3.4	6.7	5.9	21.9	24.4	21.9

FMMS: Fugl-Meyer motor scale, CR: corona radiata, PLIC: posterior limb of internal capsule.
NIHSS: National Institute of Health Stroke Scale, PVH: peri-ventricualr hyperintensity, DWMH: deep white matter hyperintensity.
[a] Median value.

2.5. Analysis of infarcted lesion

To evaluate the spatial extent of the infarction, the volume of the infarcted region was manually delineated based on the high signal contrast in the isotropic diffusion weighted image of Scan 1, and binarized and coregistered to the standard MNI space using a warping matrix. The binarized infarcted lesion area maps were summed across subjects in MNI space to generate the histogram maps of infarcted lesion. We also obtained the mean volume of the infarcted lesions in the native space (mean ± S.D., cm^3).

3. Results

3.1. Patient data

Table 1 summarizes clinical characteristics of the patients, volume of infarcted lesion, NIHSS score, Fazekas grade, time between onset and scan, and time course of FMMS score. Median Fazekas grades of periventricular and deep white matter hyperintensity were 2 and 2, respectively. The infarcted lesions were most frequently located in the posterior limb of the internal capsule (PLIC) with some upward extension to CR. Lesion overlay in the standard space is shown in Fig. 1 and the lesion location in the native space diffusion weighted image is shown in Inline Supplementary Fig. S1. The mean volume of the infarcted lesions was 1.7 ± 2.6 cm^3. The infarction volume was negatively correlated with FMMS score at the first session (Pearson's correlation $r = -0.92$, $p < 0.001$), which means that the larger the volume, the worse the motor function. This finding appears plausible because the current subjects, selected based on strict criteria, were relatively homogeneous in their symptoms and lesion locations, thus the finding may not be extrapolated to all stroke patients. The FMMS scores gradually increased, i.e., motor function was recovered, as the measured time elapsed: scores were affected by session (repeated ANOVA, $F_{2,9} = 64.0$, $p < 0.001$), and the post-hoc Tukey's test showed higher FMMS scores in the later time point ($p < 0.001$).

Inline Supplementary Fig. S1 can be found online at http://dx.doi.org/10.1016/j.nicl.2013.12.003.

3.2. Inter-hemispheric difference and time-dependent changes of FA

Voxel-based analysis with a paired *t*-test between affected and intact hemispheres at each time point of scans disclosed a significant decrease in FA in a cluster extending through the PLIC and CR of the affected hemisphere in all scan sessions, which was located within the infarcted lesion (Fig. 2A, Table 2). In Scan 3, additional clusters of decreased FA were observed in the cerebral peduncle (CP), upper part of CR, pontine part of PT, and anterior and posterior parts of corpus callosum (CC) (light-blue color in Fig. 2A, Table 2), whereas a cluster of significantly higher FA was observed in the red nucleus (c6 in Fig. 2B) and dorsal pons (c5 in Fig. 2B) ipsilateral to the infarcted lesion (see also Table 2 for coordinates of the cluster). As for the effect of time, voxel-based analysis showed lower FA in Scan 3 than in Scan 1 in CP, CR, and rostral portion and genu of CC, but this finding was at the threshold of uncorrected $p < 0.05$.

The results of ROI analysis for clusters with significant effect of hemisphere in TBSS are shown in Fig. 3. Significant effect of hemisphere was

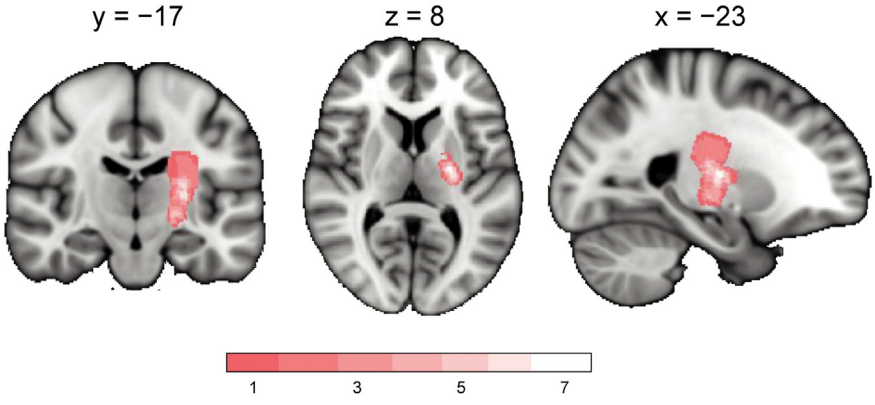

Fig. 1. Lesion overlap of the stroke patients in the current study. The lesion mask of each patient (drawn on the isotropic DWI image at Scan 1 in the native space) was warped to and overlaid on a standard MNI brain space. The number of lesions overlapped is color coded in the range of pink (n = 1) to white (n = 7).

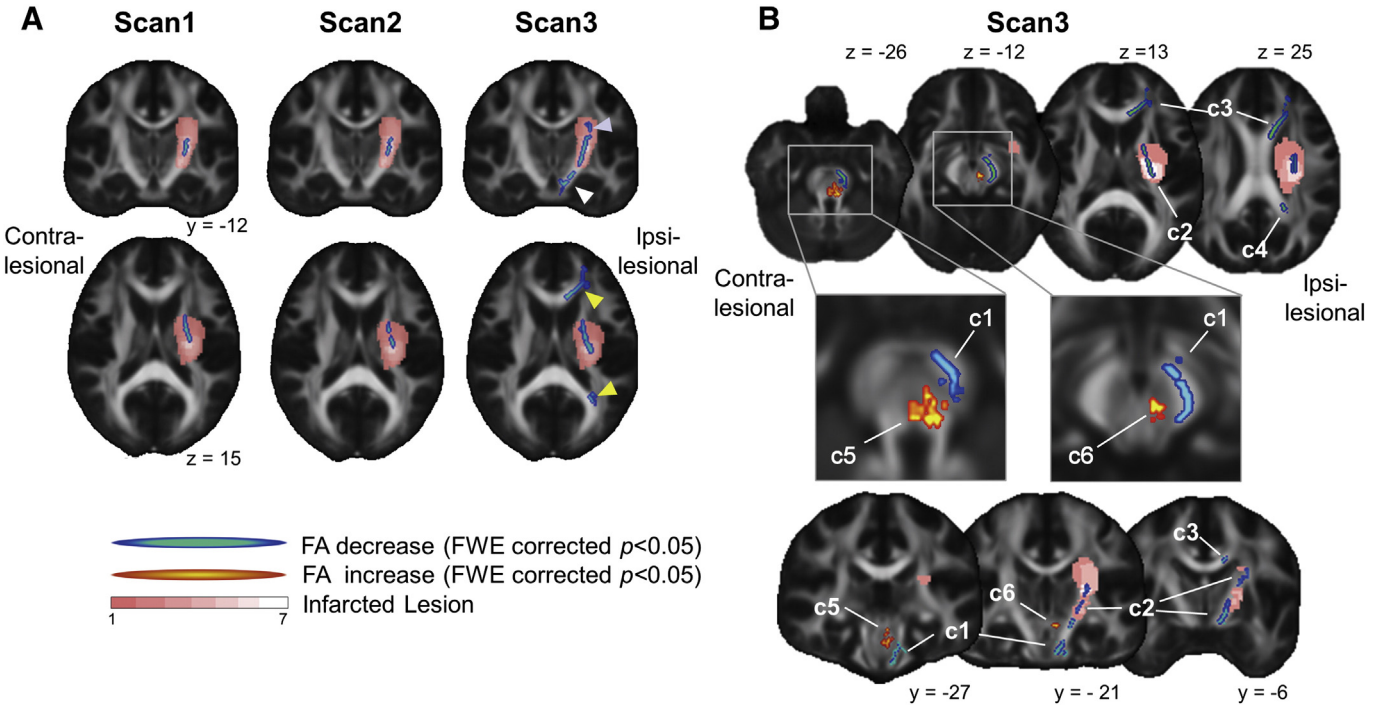

Fig. 2. Inter-hemispheric effect on FA images in TBSS. A) Inter-hemispheric FA difference between ipsi- and contra-lesional hemispheres in each scan session of Scans 1, 2, and 3. In Scans 1 and 2, significantly decreased FA (corrected $p < 0.05$, color coded in blue-green) was located mainly in the posterior limb of internal capsule (PLIC) and within a frequently infarcted region (as color coded in pink-white), whereas in Scan 3, the region of decreased FA extended distally (cerebral peduncle, white arrow head), and proximally (corona radiata, blue arrow head), and into anterior and posterior parts of the corpus callosum (yellow arrow head). B) Inter-hemispheric FA differences at Scan 3. Note that increased FA (corrected $p < 0.05$, color coded in red-yellow) was found in the dorsal pons (labeled as c5) and red nucleus (c6). Other clusters with decreased FA are labeled by: c1, cerebral peduncle (CP) through pyramidal tract (PT) of the pons; c2, PLIC through corona radiata (CR); c3, rostral parts and genu of corpus callosum (CC) and c4, isthmus of CC. Frequency of infarcted lesion is color coded by pink ($n = 1$) to white ($n = 7$). For visualization purposes, clusters were enhanced by spherical smoothing with a 1.5-mm radius. See also Table 2 for lists of clusters..

found in all the clusters at Scan 3 (paired *t*-test, $p < 0.05$), as predicted by prior TBSS analysis (Fig. 2B). Among these clusters, significant effect of scan session was found, as shown in Fig. 3, in the cluster of CP (c1, $F_{2,9} = 7.31$, $p < 0.01$), CR (c2, $F_{2,9} = 4.72$, $p < 0.05$), rostral part and genu of CC (c3, $F_{2,9} = 5.49$, $p < 0.05$), dorsal pons (c5, $F_{2,9} = 4.29$, $p < 0.05$) and the red nucleus (c6, $F_{2,9} = 4.15$, $p < 0.05$). A gradual FA decrease was found in c1, c2, and c3, whereas a time-dependent increase of FA was found in the dorsal pons (c5) and red nucleus (c6) (Fig. 3). Post-hoc analysis for sessions with the Tukey's test confirmed this trend and the FA values at Scan 3 were lower than Scan 1 and/or 2 in c1, c2, and c3 and higher than Scan 1 in the dorsal pons (c5) and red nucleus (c6).

Table 2
Statistical results of interhemispheric effect.

Session — location	Cluster label	Cluster size	MNI coordinates			t-Value
			x	y	z	
Scan1 — CR-PLIC		375	−24	−7	17	5.92¶¶
Scan2 — CR-PLIC		234	−23	−2	17	4.07¶
Scan3 — cerebral peduncle	c1	133	−8	−18	−25	5.36¶¶
Scan3 — CR-PLIC	c2	306	−24	−1	18	4.51¶
Scan3 — rostral–genu of CC	c3	706	−19	38	4	9.95¶¶
Scan3 — isthmus of CC	c4	191	−23	−50	22	5.41¶¶
Scan3 — dorsal pons	c5	76	−4	−31	−25	11.9¶¶
Scan3 — red nucleus	c6	31	−3	−27	−15	5.62¶¶

CR: corona radiata, PLIC: posterior limb of internal capsule, CC: corps callosum, I: Montreal Neurological Institute.
¶ $p < 0.05$.
¶¶ $p < 0.01$.

3.3. Correlation between FA values and FMMS scores

In the voxel-based analysis, we did not find significant clusters at the threshold of corrected $p < 0.05$. Therefore, we selected areas of interest based on the known motor network (subcortical white matter beneath motor and premotor cortices, commissural connections, motor corticospinal tracts) as well as on the prior result of inter-hemispheric effect (red nucleus/dorsal pons) and applied a threshold of uncorrected $p < 0.05$. A positive correlation was found in the midbody of CC and the cingulum of the ipsi-lesional hemisphere (Fig. 4A, Table 3), which was confirmed by ROI analysis (midbody of CC, $r = 0.513$, $p < 0.01$; cingulum, $r = 0.367$, $p < 0.05$) (Fig. 4B). ROI analysis also showed significant positive correlation of FA value in the red nucleus or dorsal pons cluster with FMMS scores (red nucleus, $r = 0.374$, $p < 0.05$; dorsal pons, $r = 0.461$, $p < 0.05$, Fig. 4B). Therefore, microstructure change in the red nucleus, dorsal pons, and midbody of the CC may underlie the reduction of motor impairment.

4. Discussion

The main findings of the present study were: (1) during a 3-month period after the onset of subcortical stroke in patients with an infarcted lesion including PT, white matter microstructure, as evaluated by FA, was gradually decreased along the CP and CR of the PT, whereas gradual increase in FA was found in the red nucleus and dorsal pons, which constitutes at least part of the rubrospinal tract; and (2) patients gradually recovered from hemiparesis, and their motor impairment, as revealed by FMMS, gradually improved during the 3-month study period and was positively correlated with FA changes in the clusters in the red nucleus, dorsal pons and the midbody of CC. These results suggest that the rubro-spinal pathway, part of the phylogenetically old EPT system,

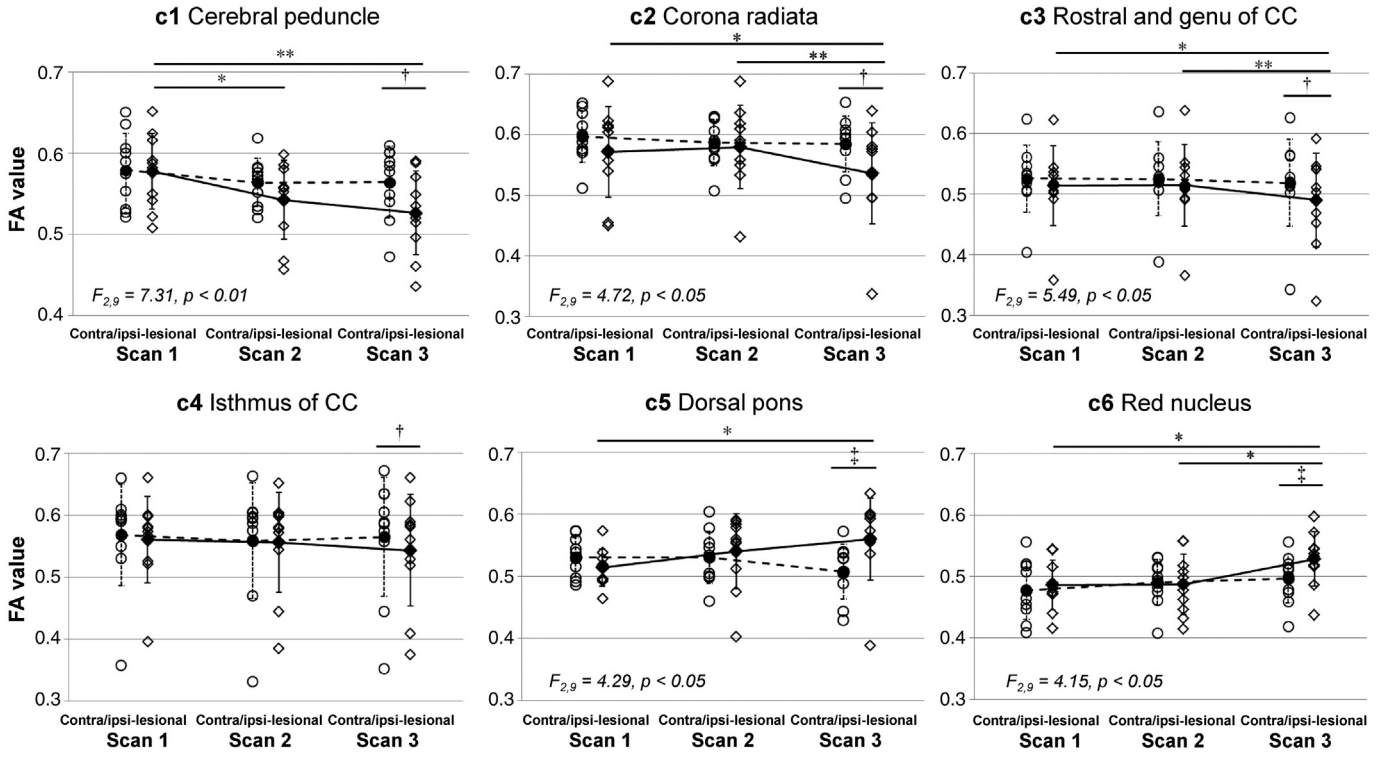

Fig. 3. Inter-hemispheric and time-dependent changes in FA in regions of interest (ROIs). Plots of FA values in clusters (c1–c6, see also Fig. 2B) and contralateral mirror regions against scan sessions (Scans 1, 2, and 3). Significant effect of scan session was found in clusters c1, c2, c3, c5 and c6 (*F*-values shown in each graph), but not in other clusters including mirror regions. $^{*}p < 0.05$, $^{**}p < 0.01$ with post-hoc Tukey's test between sessions; †$p < 0.05$, ‡$p < 0.05$ with paired *t*-test between the cluster and corresponding mirror region.

may be involved in recovery of motor function in subcortical stroke patients.

Our study indicates that microstructure of the ipsilesional red nucleus, a main location of rubro-spinal pathway, was gradually changed along with recovery of motor function after PT stroke. Longitudinal observation of FA as obtained in our study strongly suggests an association between the altered white matter microstructure and recovery of motor function. Studies in non-human primates showed that the

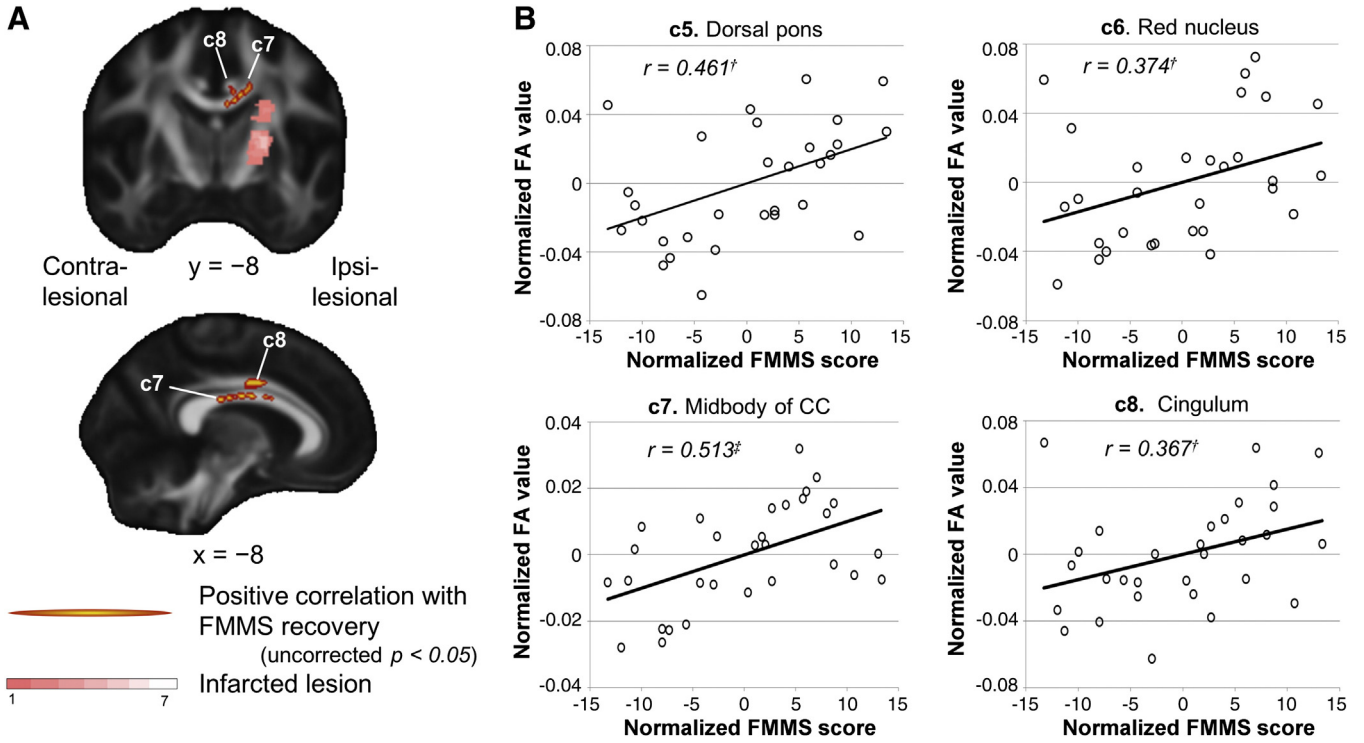

Fig. 4. Correlation of serial FA images with scores of motor function. A) Clusters with positive correlation between FA and FMMS scores (uncorrected $p < 0.05$, color coded in red-yellow) were found in midbody of CC (c7) and cingulum (c8). See also Table 3 for lists of clusters. B) Plots of FA values against FMMS scores in clusters c5, c6 (see also Fig. 2B), c7 and c8. †$p < 0.05$, ‡$p < 0.01$ with Pearson's correlation analysis.

Table 3
Positive correlation between FA and FMMS scores.

Location	Cluster label	Cluster size	MNI coordinates			t-Value
			x	y	z	
Dorsal pons	c5	76	−5	−33	−28	2.52
Red nucleus	c6	31	−6	−22	−12	2.95
Midbody of CC	c7	625	−9	6	26	4.79¶¶
Cingulum	c8	67	−8	2	35	5.17¶¶

Montreal Neurological Institute, CC: corpus callosum.
¶¶ $p < 0.01$.

rubro-spinal pathway has multi-synaptic connections to the contralateral motor neurons in the spinal cord and is involved in the movement of the distal hand, arm and fingers (Sinkjaer et al., 1995). Others also suggested a pivotal role of the rubro-spinal pathway in motor recovery after the chronic stage of PT injury in non-human primate animal models (Belhaj-Saïf and Cheney, 2000; Lawrence and Kuypers, 1968). Although the underlying mechanism of altered FA is not well understood, an increase of FA is likely associated with increased myelination or axon diameter, major constituents that limit water diffusibility in the brain tissue (Beaulieu, 2009). A previous study in normal brains showed that increased FA in the parietal white matter is associated with long-term functional plasticity (Scholz et al., 2009). This white matter change was accompanied by an increase of overlying gray matter volume of parietal cortex, which is involved in performing visuo-spatio-motor tasks. Rubro-spinal tract has been generally considered to be degraded in humans as compared with other animals (Nathan and Smith, 1955); however, there is still debate on this issue (Nudo and Frost, 2007) and a recent anatomical study indicates that a small but significant amount of rubro-spinal tract is present in the human brain (Onodera and Hicks, 2010). The functional significance of this system is also yet to be studied in humans; the current study in conjunction with previous studies (Rüber et al., 2012; Yeo and Jang, 2010) suggests that this phylogenetically old system may be important in recovering motor function after PT injury in humans.

We also found time- and recovery-dependent FA increase in the ipsilesional dorsal pons of stroke patients. The dorsal (or posterior) part of pons includes several longitudinal tracts and at least four tracts are located in this region from medial to lateral: medial longitudinal fascicles (including reticulo-spinal tract), tectospinal tract, rubro-spinal tract, and medial lemniscus (Naidich et al., 2008). The cluster found in dorsal pons (c5) in our present study may overlap any of these tracts and cannot be distinguished because of limited spatial resolution; however, the most likely candidates for functional recovery, if any, may be rubro- and reticulo-spinal tracts. The reticulo-spinal tract is a multi-synaptic connection from motor cortex to the bilateral motor neurons of spinal cord, and is considered to be involved in controlling locomotion and posture by innervating truncal and proximal limb muscles (Lemon, 2008). Since the rubro-spinal tract has been thought to be evolutionally regressed in higher mammals particularly in human, the reticulo-spinal tract is hypothesized to contribute as an alternative to recover motor function of distal limb in hemispheric injury or stroke (Baker, 2011; Bradnam et al., 2013). Interestingly, recent animal studies suggest that the reticulo-spinal tract is partially involved in hand dexterity in normal condition (Kinoshita et al., 2012), as well as in its recovery of flexor muscles after PT lesion (Zaaimi et al., 2012). Therefore, detailed studies may be needed in future to understand how much the reticulo-spinal tract contributes to the functional recovery in stroke. Potential significance of the other tracts (medial lemniscus and tectospinal tract) may also need to be addressed in future studies. Despite these unresolved issues, a recent study also showed consistent results that subcortical stroke patients with better outcome exhibited higher FA values in the dorsal pons (Wang et al., 2012).

The commissural fibers of the midbody of the CC may also be important for functional recovery. In this area, greater FA values were associated with higher FMMS scores (Fig. 4A, B). In normal human subjects, the commissural fibers of the midbody of the CC were related to bimanual coordinate motor skills (Johansen-Berg et al., 2007). In addition, in a cross-sectional study of chronic subcortical stroke patients, higher FA values in the midbody of CC were found in patients with a better functional outcome (Wang et al., 2012). Our longitudinal study confirms these observations: the infarcted lesion was mainly located in the posterior limb of the internal capsule and the FA values in the CC were increased in correlation with improvement of the motor score during the 3-month study. Because the midbody of the CC contains the commissural cortico-cortical fibers that connect bilateral sensori-motor and premotor cortices, increased FA in the commissural fibers may be related to increased functional activity in these cortical areas or/and to increased functional connectivity between these areas. Activity of the bilateral dorsal premotor cortex was shown to have a pivotal role in recovering motor function in chronic stroke patients (Fridman et al., 2004; Gerloff et al., 2006; Johansen-Berg et al., 2002) or in subjects who received transcranial magnetic stimulation that transiently inhibited the motor cortical function but maintained motor executive abilities (O'Shea et al., 2007). Commissural reorganization also supports previous studies that showed inter-hemispheric functional reorganization in animals (Nishimura et al., 2007) and in humans (Grefkes et al., 2008; Sharma et al., 2009).

We also found a significant effect of motor recovery in the middle part of the cingulum (Fig. 4A, B). The middle part of the cingulum contains motor and premotor connections (Schmahmann and Pandya, 2009), thus increased fractional anisotropy in this area may also explain a mechanism of functional recovery. Reorganization of cortico-cortical connections also supports the prior microscopic findings in studies of non-human primate animals with motor cortical lesions (Dancause et al., 2005) or with PT lesions (Higo et al., 2009).

The time-dependent gradual FA decrease found in the ipsi-lesional PT tract, in particular in the CP and CR, provides insight on the progress of Wallerian degeneration (Waller, 1850) and reproduces the findings of previous longitudinal DTI studies in stroke (Liang et al., 2007; Thomalla et al., 2004, 2005; Yu et al., 2009). Yu et al. measured DTI at five consecutive time points in subcortical stroke patients (<1 week, 2 weeks, 1 month, 3 months, 1 year), and found that the FA in the CP rapidly decreased within the first month and gradually decreased until it reached an equilibrium around 3 months after the onset. Liang et al. also showed that in some cases of subcortical stroke, decreased FA was found at 3 months and extended both distally (CP) and proximally (CR), as revealed in our TBSS analysis. Though the mechanism of decreased FA is not fully understood, in animal studies an FA decrease is clearly correlated with decreased axonal density, as revealed by immunostaining of phosphorylated neurofilaments (Hayashi et al., 2013).

Several limitations must be discussed before concluding this study. Our sample of participants with stroke was relatively small and homogenous, this may limit generalizability to the stroke population as a whole. However, our interpretation correlating rubro-spinal tract microstructural changes with motor recovery may be extrapolated to many other stroke patients, in particular, those who are affected in the corticospinal tract in the territory of middle cerebral artery, the most frequently affected major cerebral artery in stroke. Indeed, a previous study (Rüber et al., 2012) showing increased FA in the rubrospinal tract investigated stroke patients with involvement of a larger territory of the middle cerebral artery, such as the motor cortex and internal capsule.

5. Conclusion

Based on longitudinal observations, the current study demonstrated that microstructure of the rubro-spinal tract gradually changed during a period of 3 months after subcortical stroke, and this was correlated over

time with recovery of motor function. These monotonically progressive and recovery-related changes in microstructure are in contrast with those of functional activity, which were more dramatic in time, and correlated rather with initial degree of impairment than with motor recovery (Rehme et al., 2011, 2012). Our findings suggest that the viable corticofugal and inter-hemispheric connections may be recruited for functional plasticity after PT injury, and support the hypothesis that rubro-spinal pathways and cortico-cortical connections contribute to motor recovery, as derived from animal studies (Belhaj-Saïf and Cheney, 2000; Dancause et al., 2005; Lawrence and Kuypers, 1968). The results of commissural tract and cingulum also explain those of human studies that showed functional reorganization of surviving cortico-cortical networks after stroke (Grefkes et al., 2008; Sharma et al., 2009). Our findings shed light on the motor corticofugal reorganization after stroke in the pyramidal tract and opens up possibilities for the development of restorative treatments or neuromodulation (Bradnam et al., 2013; Sharma and Cohen, 2012) by targeting the presumed compensatory function of the alternative motor pathways including rubro-spinal system. Mechanisms underlying how neuromodulatory devices affect neural reorganization may also be addressed by combining with DTI.

Financial disclosures

The authors report no biomedical financial interests or potential conflicts of interest.

Acknowledgments

The authors thank Shinichi Urayama, Hiroshi Sato, and Akihide Yamamoto for their generous technical support. This study was supported by a Grant-in-Aid for Scientific Research (B) (Grant No. 24300147) of JSPS KAKENHI (T.H.).

References

Baker, S.N., 2011. The primate reticulospinal tract, hand function and functional recovery. J. Physiol. 589, 5603–5612.
Basser, P.J., Mattiello, J., LeBihan, D., 1994. MR diffusion tensor spectroscopy and imaging. Biophys. J. 66, 259–267.
Beaulieu, C., 2009. In: Johansen-Berg, H., Behrens, T. (Eds.), Diffusion MRI: From Quantitative Measurement to In Vivo Neuroanatomy. Elsevier, London.
Belhaj-Saïf, A., Cheney, P.D., 2000. Plasticity in the distribution of the red nucleus output to forearm muscles after unilateral lesions of the pyramidal tract. J. Neurophysiol. 83, 3147–3153.
Bradnam, L.V., Stinear, C.M., Byblow, W.D., 2013. Ipsilateral motor pathways after stroke: implications for non-invasive brain stimulation. Front. Hum. Neurosci. 7.
Dancause, N., Barbay, S., Frost, S.B., Plautz, E.J., Chen, D., Zoubina, E.V., Stowe, A.M., Nudo, R.J., 2005. Extensive cortical rewiring after brain injury. J. Neurosci. 25, 10167–10179.
Duncan, P.W., Goldstein, L.B., Matchar, D., Divine, G.W., Feussner, J., 1992. Measurement of motor recovery after stroke. Outcome assessment and sample size requirements. Stroke 23, 1084–1089.
Fazekas, F., Chawluk, J.B., Alavi, A., Hurtig, H.I., Zimmerman, R.A., 1987. MR signal abnormalities at 1.5 T in Alzheimer's dementia and normal aging. Am. J. Roentgenol. 149, 351–356.
Fridman, E.A., Hanakawa, T., Chung, M., Hummel, F., Leiguarda, R.C., Cohen, L.G., 2004. Reorganization of the human ipsilesional premotor cortex after stroke. Brain 127, 747–758.
Gerloff, C., Bushara, K., Sailer, A., Wassermann, E.M., Chen, R., Matsuoka, T., Waldvogel, D., Wittenberg, G.F., Ishii, K., Cohen, L.G., Hallett, M., 2006. Multimodal imaging of brain reorganization in motor areas of the contralesional hemisphere of well recovered patients after capsular stroke. Brain 129, 791–808.
Gladstone, D.J., Danells, C.J., Black, S.E., 2002. The Fugl-Meyer assessment of motor recovery after stroke: a critical review of its measurement properties. Neurorehabil. Neural Repair 16, 232–240.
Grefkes, C., Ward, N.S., 2013. Cortical reorganization after stroke: how much and how functional? Neuroscientist. http://dx.doi.org/10.1177/1073858413491147 (in press).
Grefkes, C., Nowak, D.A., Eickhoff, S.B., Dafotakis, M., Küst, J., Karbe, H., Fink, G.R., 2008. Cortical connectivity after subcortical stroke assessed with functional magnetic resonance imaging. Ann. Neurol. 63, 236–246.
Hayashi, T., Shimazawa, M., Watabe, H., Ose, T., Inokuchi, Y., Ito, Y., Yamanaka, H., Urayama, S., Watanabe, Y., Hara, H., Onoe, H., 2013. Kinetics of neurodegeneration based on a risk-related biomarker in animal model of glaucoma. Mol. Neurodegener. 8, 4.
Higo, N., Nishimura, Y., Murata, Y., Oishi, T., Yoshino-Saito, K., Takahashi, M., Tsuboi, F., Isa, T., 2009. Increased expression of the growth-associated protein 43 gene in the sensorimotor cortex of the macaque monkey after lesioning the lateral corticospinal tract. J. Comp. Neurol. 516, 493–506.
Jenkinson, M., Beckmann, C.F., Behrens, T.E.J., Woolrich, M.W., Smith, S.M., 2012. FSL. NeuroImage 62, 782–790.
Johansen-Berg, H., Rushworth, M.F., Bogdanovic, M.D., Kischka, U., Wimalaratna, S., Matthews, P.M., 2002. The role of ipsilateral premotor cortex in hand movement after stroke. Proc. Natl. Acad. Sci. 99, 14518–14523.
Johansen-Berg, H., Della-Maggiore, V., Behrens, T.E., Smith, S.M., Paus, T., 2007. Integrity of white matter in the corpus callosum correlates with bimanual co-ordination skills. NeuroImage 36 (Suppl. 2), T16–T21.
Kelly-Hayes, M., Wolf, P.A., Kase, C.S., Gresham, G.E., Kannel, W.B., D'Agostino, R.B., 1989. Time course of functional recovery after stroke: the Framingham study. Neurorehabil. Neural Repair 3, 65–70.
Kinoshita, M., Matsui, R., Kato, S., Hasegawa, T., Kasahara, H., Isa, K., Watakabe, A., Yamamori, T., Nishimura, Y., Alstermark, B., Watanabe, D., Kobayashi, K., Isa, T., 2012. Genetic dissection of the circuit for hand dexterity in primates. Nature 487, 235–238.
Lawrence, D.G., Kuypers, H.G., 1968. The functional organization of the motor system in the monkey. II. The effects of lesions of the descending brain-stem pathways. Brain 91, 15–36.
Lemon, R.N., 2008. Descending pathways in motor control. Annu. Rev. Neurosci. 31, 195–218.
Liang, Z., Zeng, J., Liu, S., Ling, X., Xu, A., Yu, J., Ling, L., 2007. A prospective study of secondary degeneration following subcortical infarction using diffusion tensor imaging. J. Neurol. Neurosurg. Psychiatry 78, 581–586.
Lindenberg, R., Renga, V., Zhu, L.L., Betzler, F., Alsop, D., Schlaug, G., 2010. Structural integrity of corticospinal motor fibers predicts motor impairment in chronic stroke. Neurology 74, 280–287.
Mori, S., Crain, B.J., 2005. MRI Atlas of Human White Matter. Elsevier, Amsterdam; Boston.
Naidich, T.P., Duvernoy, H.M., Delman, B.N., Sorensen, A.G., Kollias, S.S., Haacke, E.M., 2008. Duvernoy's atlas of the human brain stem and cerebellum: high-field MRI, surface anatomy, internal structure, vascularization and 3 D sectional anatomy, 1st ed. Springer.
Nathan, P.W., Smith, M.C., 1955. Long descending tracts in man. I. Review of present knowledge. Brain 78, 248–303.
Nishimura, Y., Onoe, H., Morichika, Y., Perfiliev, S., Tsukada, H., Isa, T., 2007. Time-dependent central compensatory mechanisms of finger dexterity after spinal cord injury. Science 318, 1150–1155.
Nudo, R.J., Frost, S.B., 2007. 3.28 — the evolution of motor cortex and motor systems. Evolution of Nervous Systems. Academic Press, Oxford, pp. 373–395.
O'Shea, J., Johansen-Berg, H., Trief, D., Gobel, S., Rushworth, M.F., 2007. Functionally specific reorganization in human premotor cortex. Neuron 54, 479–490.
Onodera, S., Hicks, T.P., 2010. Carbocyanine dye usage in demarcating boundaries of the aged human red nucleus. PLoS ONE 5.
Rehme, A.K., Fink, G.R., von Cramon, D.Y., Grefkes, C., 2011. The role of the contralesional motor cortex for motor recovery in the early days after stroke assessed with longitudinal FMRI. Cereb. Cortex 1991 (21), 756–768.
Rehme, A.K., Eickhoff, S.B., Rottschy, C., Fink, G.R., Grefkes, C., 2012. Activation likelihood estimation meta-analysis of motor-related neural activity after stroke. NeuroImage 59, 2771–2782.
Rüber, T., Schlaug, G., Lindenberg, R., 2012. Compensatory role of the cortico-rubro-spinal tract in motor recovery after stroke. Neurology 79, 515–522.
Schmahmann, J.D., Pandya, D.N., 2009. Fiber Pathways of the Brain, 1st ed. Oxford University Press, USA.
Scholz, J., Klein, M.C., Behrens, T.E., Johansen-Berg, H., 2009. Training induces changes in white-matter architecture. Nat. Neurosci. 12, 1370–1371.
Sharma, N., Cohen, L.G., 2012. Recovery of motor function after stroke. Dev. Psychobiol. 54, 254–262.
Sharma, N., Baron, J.-C., Rowe, J.B., 2009. Motor imagery after stroke: relating outcome to motor network connectivity. Ann. Neurol. 66, 604–616.
Sinkjaer, T., Miller, L., Andersen, T., Houk, J., 1995. Synaptic linkages between red nucleus cells and limb muscles during a multi-joint motor task. Exp. Brain Res. 102.
Smith, S.M., Nichols, T.E., 2009. Threshold-free cluster enhancement: addressing problems of smoothing, threshold dependence and localisation in cluster inference. NeuroImage 44, 83–98.
Smith, S.M., Jenkinson, M., Johansen-Berg, H., Rueckert, D., Nichols, T.E., Mackay, C.E., Watkins, K.E., Ciccarelli, O., Cader, M.Z., Matthews, P.M., Behrens, T.E.J., 2006. Tract-based spatial statistics: voxelwise analysis of multi-subject diffusion data. NeuroImage 31, 1487–1505.
Stinear, C.M., Barber, P.A., Smale, P.R., Coxon, J.P., Fleming, M.K., Byblow, W.D., 2007. Functional potential in chronic stroke patients depends on corticospinal tract integrity. Brain 130, 170–180.
Thomalla, G., Glauche, V., Koch, M.A., Beaulieu, C., Weiller, C., Rother, J., 2004. Diffusion tensor imaging detects early Wallerian degeneration of the pyramidal tract after ischemic stroke. NeuroImage 22, 1767–1774.
Thomalla, G., Glauche, V., Weiller, C., Röther, J., 2005. Time course of Wallerian degeneration after ischaemic stroke revealed by diffusion tensor imaging. J. Neurol. Neurosurg. Psychiatry 76, 266–268.
Veerbeek, J.M., Kwakkel, G., van Wegen, E.E.H., Ket, J.C.F., Heymans, M.W., 2011. Early prediction of outcome of activities of daily living after stroke: a systematic review. Stroke 42, 1482–1488.
Waller, A., 1850. Experiments on the section of the glossopharyngeal and hypoglossal nerves of the frog, and observations of the alterations produced thereby in the structure of their primitive fibres. Philos. Trans. R. Soc. Lond. 140, 423–429.
Wang, L.E., Tittgemeyer, M., Imperati, D., Diekhoff, S., Ameli, M., Fink, G.R., Grefkes, C., 2012. Degeneration of corpus callosum and recovery of motor function after

stroke: a multimodal magnetic resonance imaging study. Hum. Brain Mapp. 33, 2941–2956.
Witelson, S.F., 1989. Hand and sex differences in the isthmus and genu of the human corpus callosum. A postmortem morphological study. Brain 112, 799–835.
Yeo, S.S., Jang, S.H., 2010. Changes in red nucleus after pyramidal tract injury in patients with cerebral infarct. NeuroRehabilitation 27, 373–377.
Yu, C., Zhu, C., Zhang, Y., Chen, H., Qin, W., Wang, M., Li, K., 2009. A longitudinal diffusion tensor imaging study on Wallerian degeneration of corticospinal tract after motor pathway stroke. NeuroImage 47, 451–458.
Zaaimi, B., Edgley, S.A., Soteropoulos, D.S., Baker, S.N., 2012. Changes in descending motor pathway connectivity after corticospinal tract lesion in macaque monkey. Brain 135, 2277–2289.